



Characteristics of the monsoon low pressure systems in the Indian subcontinent and the associated extreme precipitation events

Tresa Mary Thomas¹ · Govindasamy Bala^{1,2} · Vemavarapu Venkata Srinivas^{1,3}

Received: 25 May 2020 / Accepted: 26 November 2020 / Published online: 2 January 2021
© The Author(s), under exclusive licence to Springer-Verlag GmbH, DE part of Springer Nature 2021

Abstract

The South Asian summer monsoon brings copious rain to agriculture-dependent country India and bulk of the precipitation in central India is attributed to monsoon low pressure systems (LPS). Large uncertainty exists in the statistics of LPS during the historical period and in future projections. In this study, we have developed an LPS tracking approach which considers geopotential height anomaly and relative vorticity thresholds. The approach is validated by comparing characteristics of LPS from our tracking scheme with those from previous studies. Our analysis indicates around 14 LPS per year (over 68 LPS-days). 60–70% of monsoon rainfall in north, east and central India is found to be associated with LPS (location is within 1000 km radii of LPS). Over the central Indian region, around 82% of extreme precipitation events occur during LPS days, out of which 47% are on depression and deep depression days and 78% is associated with LPS. 15–25% of monsoon precipitation in central and East Indian states is in the form of extreme precipitation associated with LPS. At many locations in central India, very heavy precipitation (≥ 124.5 mm/day) due to LPS is estimated to have a return period less than 5 years. Further, our analysis shows that the intensity of extreme precipitation is larger by 50% (95th percentile precipitation) to 100% (99th percentile) when the extreme is associated with LPS. Our analysis of extreme precipitation related to LPS has the potential to provide valuable information for flood risk assessment during monsoon season in central India.

Keywords Indian summer monsoon · Monsoon low pressure systems · LPS tracks · Extreme precipitation events

1 Introduction

For millions of people inhabiting the mainland of India, monsoon is more than a lifeline, as more than 50 percent of the population depends on monsoon precipitation for agriculture and economic growth (Saha et al. 1979). Spanning through the months of June to September, Indian monsoon contributes about 80 percent of the annual precipitation for

the country. Considered initially as a large land–sea breeze (Webster 1987), further research has indicated that the monsoon is a manifestation of seasonal migration of Inter tropical convergence zone (ITCZ) over the Indian subcontinent. The migration occurs in response to variation in the latitude of maximum solar insolation (Gadgil 2003) which causes a reversal of the wind over the Indian land mass that brings in copious amounts of water vapor all the way from southern hemisphere during the boreal summer.

A significant part of monsoon precipitation in the core monsoon region of India (central India) is attributed to synoptic scale tropical disturbances called low pressure systems (LPS) (Sikka 1980), which usually form during the southwest monsoon season mostly over the warm waters of Bay of Bengal (BoB) and propagate northwestward along the monsoon trough. Some LPS may also form over east Arabian sea and over land, but they constitute less than 20 percent of the total number of systems (Krishnamurthy and Ajayamohan 2010). Monsoon LPS are attributed to produce around 57% of monsoon precipitation over core monsoon region of India

Supplementary Information The online version contains supplementary material available at <https://doi.org/10.1007/s00382-020-05562-2>.

✉ Tresa Mary Thomas
tresathomas@iisc.ac.in

¹ Interdisciplinary Centre for Water Research, Indian Institute of Science, Bangalore, India

² Centre for Atmospheric and Oceanic Sciences, Indian Institute of Science, Bangalore, India

³ Civil Engineering, Indian Institute of Science, Bangalore, India

and 44% of monsoon precipitation for the country (Hunt and Fletcher 2019).

Some of the necessary conditions for the formation of LPS are large sea surface temperature, presence of monsoon trough over north BoB, and moist and unstable atmosphere. Energy for the initial stage is provided by barotropic dynamics, while in the later stages baroclinic instability and convective instability of second kind are supposed to provide the major energy (Sikka 1977; Keshavamurty et al. 1978). The northwest propagation of LPS is regarded as a response to the feedback mechanism of cumulus convection coupled with maxima of low-level cyclonic vorticity. The initial cyclonic vorticity induces cumulus convection that releases latent heat which in turn acts as a heat source in the troposphere. The atmospheric response to such a heat source is in the form of Rossby gravity wave propagation towards the west. This Rossby gravity wave in turn produces a strong low-level cyclonic vorticity which leads to cumulus convection on the north-west quadrant leading the system to move towards north-west direction (Goswami 1987; Chen et al. 2005). Further studies show that in the later stages of LPS, wind-induced surface heat exchange which causes amplification of tropical cyclones is a major energy source (Diaz and Boos 2019). But strong vertical wind shear prevents these systems to further intensify into tropical cyclones. An alternate mechanism for monsoon LPS propagation considers LPS as mid tropospheric potential vorticity (PV) maxima which propagate by adiabatic beta drift (Boos et al. 2015). The mid tropospheric PV maximum lies southwest of the low-level PV maximum and its vertical advection and diabatic heating tries to shift the low-level PV maximum to south-west of its original location. But horizontal advection tries to shift the low-level PV maximum to north-northwest. The super-position of these two motions results in north-west propagation of PV maximum and hence the LPS (Boos et al. 2015; Hunt and Parker 2016).

India Meteorological Department (IMD) classifies LPS into various categories, depending on the minimum surface pressure and the maximum wind speed along its track

(Table 1). The weaker systems are called lows and stronger systems are categorized as depressions, deep depressions, cyclonic storms, and severe cyclonic storms (IMD 2003). During the monsoon season, these systems do not intensify into intense tropical cyclones mainly because of their small lifetime over ocean and strong vertical wind shear (Krishnamurthy and Ajayamohan 2010). In our analysis, we exclude tropical cyclones, and we classify LPS into three categories, namely, lows, depressions and relatively stronger deep depressions (Table 1). Earlier studies have shown that around 14 systems form every year with about half of them being depressions (Mooley and Shukla 1987). The lifetime of these systems is around 2–5 days (Sikka 1977). They move northwestward at a speed of around 170 km/day and have a horizontal size of around 1000–2000 km (Mooley and Shukla 1987; Sikka 1977; Dhar and Nandargi 1999). They have an intense closed vortex in the lower levels with a warm core above cold core extending to a height of around 9 km (Krishnamurti et al. 1975).

Indian Monsoon LPS have been extensively studied through the years. One of the pioneers of this area of study is Dr. Sikka, who carefully examined sea level synoptic pressure charts published by IMD and developed a dataset comprising information on genesis, tracks and intensity of all LPS formed during 1984–2003. The “Sikka’s archive”, covers the period 1883–2003. It comprises tracks compiled by Mooley and Shukla (1987) for the period 1888–1983 and by Sikka (2006) for the period 1984–2003. Sikka’s archive has formed the basis for all further analysis. Various studies (Sikka 2006; Ajayamohan et al. 2010) have attempted to develop approaches to understand the mechanism of formation and propagation of LPS, and to analyze their statistics. Some of these studies have found a significant decline in the number of depressions that formed over the Indian subcontinent during the recent decades (Sikka 2006; Patwardhan and Bhalme 2001; Mandke and Bhade 2003; Prajesh et al. 2013). Interestingly, later studies (Cohen and Boos 2014) using satellite and reanalysis (ERA-Interim) data products did not show any significant decline in the number of

Table 1 Criteria considered by different algorithms to classify LPS into lows, depressions and deep depressions

(a) Criteria in case of HB2015 and IMD archives

	Lows	Depressions	Deep depressions
Sea level pressure Anomaly	2–4 hPa	4–10 hPa	>10 hPa
Wind at 10 m	–	8.5–13.5 m/s	>13.5 m/s

(b) Criteria in case of ATAGC algorithm

	Lows	Depressions	Deep depressions
Geopotential Anomaly at 850 hPa	< – 120 m ² /s ² – – 250 m ² /s ²	– 250 m ² /s ² – – 500 m ² /s ²	< – 500 m ² /s ²
Wind at 850 hPa	–	8.5–13.5 m/s	>13.5 m/s

depressions in the past 30 years. An automated LPS tracking algorithm when applied on ERA-Interim data identified multiple tracks which IMD had missed in the recent past (Cohen and Boos 2014). Similar tracking algorithms have been now developed and applied on various reanalysis data products (Hurley and Boos 2015; Praveen et al. 2015; Hunt et al. 2016; Vishnu et al. 2020) to understand the synoptic features of LPS. Attempts have also been made to understand likely change in characteristics of these systems by studying their future projections under various climate change scenarios (Sandeep et al. 2018; Rastogi et al. 2018; Sørland and Sorteberg 2016) using climate models.

Different reanalysis products and tracking algorithms have been used in the literature (e.g. Hurley and Boos 2015; Praveen et al. 2015; Vishnu et al. 2020) to determine genesis points and tracks of LPS over the Indian subcontinent. But none of the algorithms was able to yield results which are consistent with observations of IMD on the year-to-year variability of number of LPS. Storm counts are known to deviate to a large extent depending on the algorithm used for the objective tracking of LPS (Cohen and Boos 2014; Vishnu et al. 2020). The inconsistency could be partly attributed to subjectivity involved in factors (e.g., thresholds for minimum vorticity, wind speed, minimum sea level pressure or geopotential height and minimum duration of LPS) used for identification and tracking of LPS by IMD and other studies. Also, there are differences between these algorithms in the methodology used for determining the genesis points and tracks of LPS. Uncertainty can also arise due to differences in the reanalysis data products (e.g., Praveen et al., 2015). This is evaluated in a recent study (Vishnu et al. 2020) by considering 2048 track sets produced from four reanalysis data products by varying the magnitude of different parameters and thresholds in the tracking algorithm called TempestExtremes. The algorithm is reported to capture monthly and basin-wide LPS climatology using some of the reanalysis products and related track sets. Nevertheless, correlation for inter-annual variations of monsoon LPS count between reanalysis data products is reported to be small. Consequently, inconsistency exists between count and characteristics of LPS derived using the algorithms for both the past and future periods. We believe there is a need for further research to enhance our understanding of the large-scale factors which influence the intensity, frequency and tracks of these LPS in order to determine reliable estimates of the spatial pattern of monsoon precipitation in the Indian subcontinent.

Many extreme precipitation events in the Indian subcontinent are attributed to LPS. Several studies have reported an increase in extreme precipitation events over India during the past few decades (Rajeevan et al. 2008). The evidence of an increase in extreme precipitation events coupled with decrease in depressions (e.g., Sikka 2006) was a puzzle.

Later, it was found that the extreme precipitation events were not influenced by depressions alone, but also by lows (weaker systems) which show an increasing trend consistent with that of extreme events (Ajayamohan et al. 2010).

If extreme precipitation events occurring within 5° of LPS tracks are attributed to LPS, around 62% of extreme precipitation events in central India are found to be LPS related (Ajayamohan et al. 2010) during the period 1951–2003 in analysis based on LPS tracks in Sikka archive and 1° × 1° gridded IMD precipitation data. However, estimation of local scale extreme precipitation characteristics associated with LPS has not received attention in previous studies. We attempt to address this research gap in this paper, as it would help us to better prepare to cope with future extreme precipitation events by devising appropriate water management and flood mitigation strategies. To achieve this objective, an alternate algorithm/methodology to track LPS in the Indian subcontinent is suggested by considering geopotential height at 850 mb as a key variable. Development of the algorithm is motivated by the fact that the existing LPS databases do not permit establishing superiority of any one of the existing tracking algorithms, as knowledge on true LPS tracks is unavailable. Investigations are carried out to verify if the developed algorithm yields LPS tracks whose characteristics are closer to those of tracks available from existing algorithms and other LPS datasets. Once we are satisfied that our algorithm is reasonably consistent with the existing ones, we analyze statistics of the tracked LPS and the related extreme precipitation events.

The remainder of this paper is organized as follows. Section 2 presents a brief description of the methodology/algorithm developed to identify LPS genesis points and tracks. Section 3 describes the study area and data used for the analysis. Section 4 provides a detailed analysis of the performance of the new algorithm when applied to ERA-Interim data. Estimates are also given for characteristics of extreme precipitation events, both in terms of frequency of events and magnitude of extreme precipitation. Section 5 provides the summary and conclusions drawn from the analysis.

2 Methodology

For tracking of LPS using gridded atmospheric data, a new automated approach is developed by adapting algorithm developed by Hodges (1994). It is henceforth referred to as Automated Tracking Algorithm using Geopotential Criteria (ATAGC). Following Hodges (1994), the analysis is performed at 850 hPa level to avoid the influence of topography, and considering relative vorticity as a key climate variable for tracking of LPS. Geopotential height is suggested as an additional key variable in this study. Previous studies (Hunt et al. 2016; Sørland and Sorteberg 2016) have used sea level

pressure as the additional key variable. Since sea level pressure estimates are prone to errors over land, specially near mountainous regions (Nigam and Baxter 2015), we opted to use geopotential height anomaly at 850 hPa in our analysis. Relative vorticity and geopotential height data were used at a horizontal resolution of $0.75^\circ \times 0.75^\circ$ and $3^\circ \times 3^\circ$ (regridded from $0.75^\circ \times 0.75^\circ$ grids) respectively. For categorizing LPS, horizontal wind speed at 3° resolution is considered. Tracking of LPS is performed using relative vorticity, while presence of low pressure in an area is confirmed using geopotential height anomaly with respect to its surroundings. The anomalies are estimated at a coarser resolution, as LPS is a large-scale feature.

The tracking algorithm can be divided into three parts: segmentation, feature point detection, and tracking.

Segmentation: Segmentation is basically thresholding/classification of grids (locations) in the study area into object points and background points using information on relative vorticity (Fig. S1). Object points denote possible locations of LPS, and all other points are referred to as background points. A location is considered as an object point if relative vorticity at the location is greater than a threshold, which is chosen as $0.5 \times 10^{-5} \text{ s}^{-1}$ in this study following Hodges (1994). Object points are assigned a value 1 and background points are assigned a value 0. Thus, for a given time frame, the study area can be represented as a matrix comprising of zeros and ones as shown in Fig. S1.

Object points which are connected to each other can represent a single system and are referred to as object class. In this study, object classes are identified using connected compound labeling algorithm (Samet 1981). The algorithm assigns a common label to object points whose edges or corners are connected to each other, thus representing them as a single system. Following this, it resolves the equivalences. In other words, if a single object point has more than one label (e.g., two labels), then object classes with different labels are merged together to represent a single object class which is given a unique label. Thus, all object points belonging to a distinct system or object class are uniquely labeled. In Fig. S1(b), the boxes indicate uniquely identified object classes for a typical time frame.

Feature point detection: In the traditional algorithm (Hodges 1994), after identifying an object class for a given time frame, the object point(s) having the largest value of relative vorticity is (are) considered as feature point(s). Instead, the algorithm developed in this paper proposes plotting contours of relative vorticity inside each object class to identify utmost six peaks as potential locations of feature points as shown in Fig. S2. The peaks which are more than 3° apart (since geopotential height anomalies are used at 3° resolution) are considered as different feature points within the object class for the given time frame. For determining the strength of a feature point, clustering analysis

using Euclidean distance method (Hodge 1994) is adopted. The object points inside each object class are delineated into clusters such that each cluster has feature point as its cluster center. Strength of each feature point is calculated as the average of relative vorticity values of the object points found in the cluster corresponding to the feature point.

Another variation that has been made in the proposed algorithm is the use of geopotential height anomaly criteria. Geopotential height anomaly is determined at each location by subtracting the average of geopotential height values at the surrounding eight locations from the geopotential height value at the location (Fig. S3). If the geopotential anomaly at a location is less than a threshold ($-120 \text{ m}^2/\text{s}^2$), then the feature point in that location is considered (as a positive location) for further analysis. The geopotential anomaly threshold is based on IMD guideline for declaring an LPS (Table 1b).

Tracking: A given time frame has a set of feature points in each object class. Feature points in consecutive time frames (6 h apart) are linked using nearest neighbor distance method. Feature points in consecutive time frames which are less than 6° apart are considered to be the locations of same LPS at consecutive time frames. The process is repeated for consecutive time frames and tracks are obtained. If the neighbor of a feature point in a given time frame is not found in its next time frame, the algorithm searches for neighbor in consecutive time frames up to 1 day (to account for occlusion). The upper bound of 6° is decided based on the maximum possible distance travelled by LPS in 24 h in observations (average distance being around $\sim 2^\circ$ in a day).

In Hodges (1994) algorithm, a cost function comprising of distance and direction between three consecutive feature points is minimized to obtain the final track. This is necessary when only relative vorticity is used for tracking LPS and multiple feature points exist at a given time frame. Since our algorithm (ATAGC) uses geopotential criteria also, only those feature points which satisfy both relative vorticity and geopotential criteria are considered for tracking LPS. Hence a selected few feature points exist at a given time frame and the implementation of the minimization of cost function is not needed in the algorithm. Even when the minimization of cost function was used, we found that the tracks obtained did not vary much with respect to those obtained without the use of cost function.

The ATAGC algorithm is designed to identify only those tracks which last for more than 2 days. The distinction between lows, depressions and deep depressions is made from a combination of geopotential height anomaly criteria and wind criteria (Table 1). Information on maximum wind speed within 5° radius around each feature point is extracted for the entire lifetime of the system. The largest of such maxima extracted for a track is used for classifying LPS into lows, depressions and deep depressions.

To avoid classifying tropical cyclones as LPS in our analysis, an extra filter is applied. Tropical cyclones are associated with maximum wind speeds which are larger than those corresponding to depressions. Hence, the filter is applied to only deep depressions with genesis over ocean. Tropical cyclones have a warm core throughout, while monsoon LPS have a warm over cold core. Therefore, temperature anomaly at 900 hPa is used for filtering out tropical cyclones. If the temperature anomaly (relative to the surrounding 8 grid points of 0.75° resolution) along the track is found to be greater than zero, then presence of warm core is established, and the deep depression is considered to be a tropical cyclone which is then excluded from our analysis.

3 Study area and data used

The study area (Fig. 1) has the longitudinal extent of 60° E– 100° E and latitudinal extent of 5.25° N– 28.5° N and it includes the Indian subcontinent. The area encompasses the genesis region of LPS in the north Indian Ocean and their tracks evident from the literature. While tracking LPS, if a system crosses the boundary of the study area, it is tracked till its termination point. To reduce the influence of the Himalayas (Hunt et al. 2016), the Himalayan regions in Nepal, Uttarakhand and Arunachal Pradesh are not included in the study area while tracking LPS.

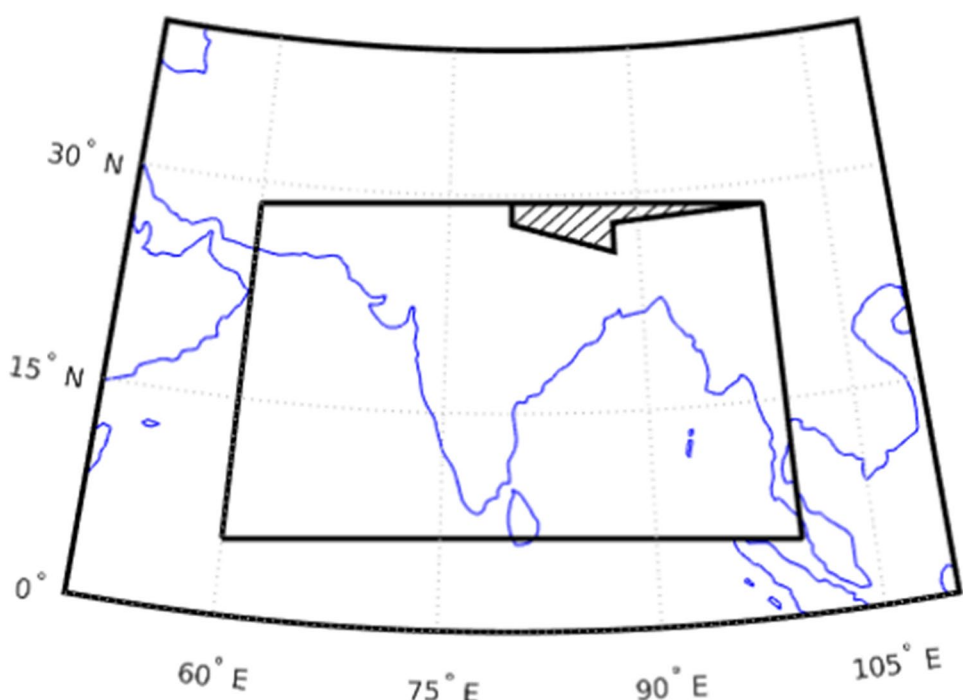
To determine tracks of LPS using ATAGC, $0.75^\circ \times 0.75^\circ$ resolution gridded ERA-Interim data produced by the European Center for Medium Range Forecasts are used

(Dee et al. 2011). Datasets for geopotential height, relative vorticity and surface horizontal wind speeds at 850 hPa pressure level for the summer monsoon months (June–September) are obtained at 6 hourly time scale for the period 1979–2015. Recently, a new version of the ERA reanalysis dataset (ERA5) is made available (Hersbach and Dee 2016; Hersbach et al. 2019). However, LPS datasets available from previous studies (e.g. Hurley and Boos 2015) were derived using ERA-Interim reanalysis data. Hence, to facilitate comparing performance of the newly proposed ATAGC algorithm with those of the existing algorithms, we have considered ERA-Interim data.

LPS tracks which pass through our study area are also obtained from the Global monsoon disturbance track dataset (Hurley and Boos 2015) for the time period 1979–2012 for the purpose of comparison with tracks generated using ATAGC. For brevity, we refer to this dataset as HB2015. We also use Cyclone eAtlas provided by IMD. The atlas comprises of tracks of depressions and deep depressions for the period 1891–2003 and does not include the weaker systems (called lows). These are hereafter referred as IMD tracks. They are compared with those obtained using ATAGC for the overlapping period of 1979–2003.

Apart from the eAtlas, IMD publishes a detailed report every year called ‘Mausam’, which discusses the monsoon activity in the country. Location of LPS tracks extracted from this report for the latest years (2010–2015) are also used in our analysis. In addition, data are extracted on genesis, tracks and intensity of all LPS during 1979–2003 from Sikka’s archive (Sikka 2006). It should be noted that the

Fig. 1 Area of study. The inner domain (with longitudinal boundary of 60° E– 100° E and latitudinal boundary of 5.25° N– 28.5° N) shows the region where the tracking of LPS is performed. It comprises of the major locations of formation and propagation of LPS in the Indian subcontinent. To avoid the influence of Himalayas, while tracking, the hatched polygonal region in Himalayas comprising Nepal (country) and Arunachal Pradesh (state in India) is excluded from the study area



Sikka's archive, as discussed earlier, refers to the combined compiled set of LPS tracks during 1888–1983 (Mooley and Shukla 1987) and 1984–2003 (Sikka 2006). Earlier studies (Krishnamurthy and Ajayamohan 2010) have constructed track climatology using the entire record (1888–2003) but we use the track information corresponding to the period 1979–2003 in this study.

To analyze the dependence of LPS on ENSO, Nino 3.4 index (SST anomaly in the Nino 3.4 region) are obtained for the period 1979–2015 at monthly scale from National Oceanic and Atmospheric Administration (<https://www.cpc.ncep.noaa.gov/data/indices>). Since extreme precipitation effects are observed at finer spatial scales, we have performed extreme precipitation analysis at 0.25° resolution using IMD daily gridded data (Rajeevan 2006) for the 37 years (1979–2015) period. Several previous studies (Goswami et al. 2006; Ajayamohan et al. 2010) have also used IMD data for analysis of precipitation and its extremes over Indian subcontinent. Further, IMD data are found to be consistent with precipitation records available from TRMM (Tropical Rainfall Measuring Mission) for the common period 1989–2015 (Prakash et al. 2014). Since sub-daily gridded precipitation data are unavailable with IMD, precipitation data at sub-daily (3-hourly) scale obtained from TRMM 3B42V7 are used for analysis of rainfall spells.

4 Results and discussion

Our tracking algorithm ATAGC is applied on ERA-Interim data product to produce tracks of LPS for the period 1979–2015. Various features of those tracks are compared with features of LPS tracks extracted from IMD annual reports, Sikka's archive and HB2015 to validate ATAGC. Following this, precipitation associated with the tracks from ATAGC are analyzed to assess statistics of extreme precipitation characteristics associated with LPS.

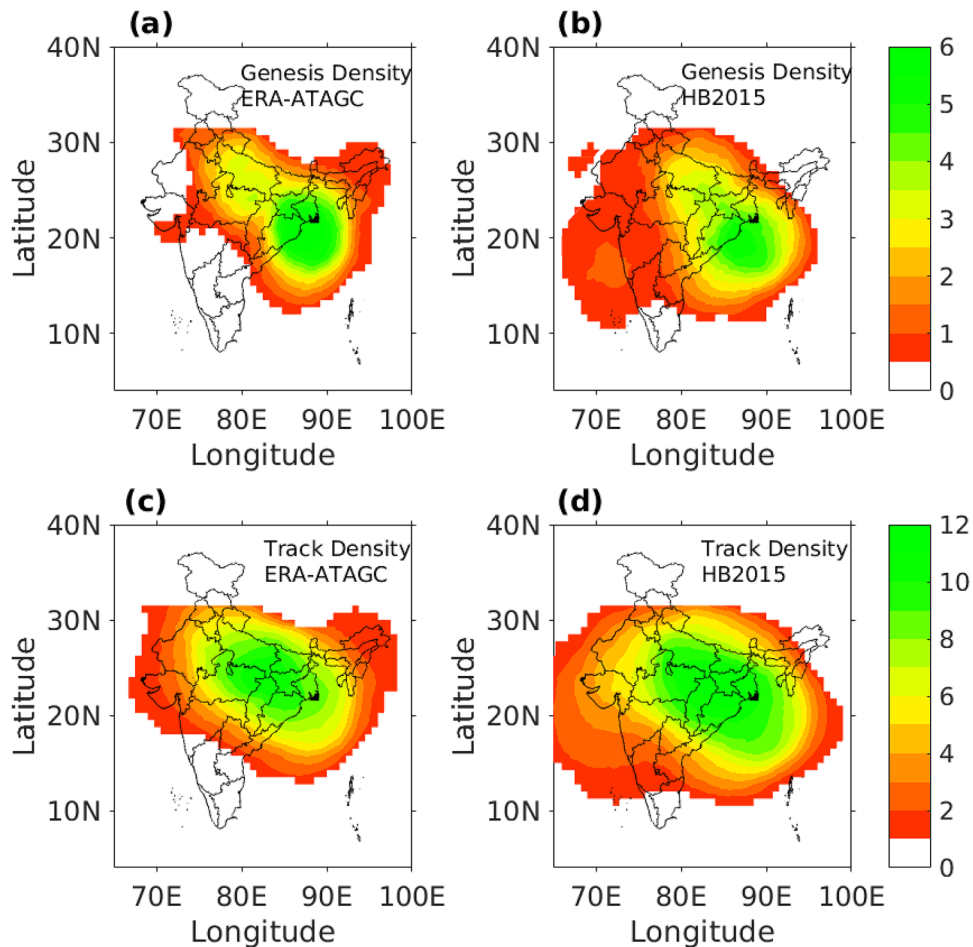
4.1 Genesis locations and tracks

LPS in the Indian subcontinent mostly form over northern part of BoB and move northwestward. In the literature, differences are noted in estimates of frequency of LPS and the number of days on which LPS are observed in the study area (i.e., LPS days). Sikka's archive indicates that on an average around 13 systems formed in a year during 1888–2003, and generally 59 out of 122 days of the monsoon period (June–September) are LPS days (Krishnamurthy and Ajayamohan 2010). However, HB2015 indicates around 16 LPS and 90 LPS days per year during 1979–2012. On the other hand, our analysis indicates around 14 LPS and 68 LPS days per year. The genesis and tracks considered in our analysis are shown in Fig. S4.

Figure 2a shows the LPS genesis density (number of genesis per year within 500 km of each grid location) obtained by applying ATAGC on ERA-Interim data. A maximum of around 6 LPS form every year along the core monsoon genesis region of northern BoB. Similar result is also obtained while analyzing the tracks of HB2015 (Fig. 2b). The maximum of genesis density in the core genesis region of BoB is about 12 LPS per summer in Sikka's archive (Hurley and Boos 2015). However, the genesis area (i.e., area over which genesis occurs) in our analysis and HB2015 is larger than that in the case of the Sikka archive, so that the area integrals (over incremental area equal to $\pi(500)^2 \text{ km}^2$) of genesis density are nearly the same. These differences are likely because of the differences in methodologies adopted. Genesis points in Sikka's archive are determined by subjective analysis of sea level pressure maps, while those in HB2015 are obtained by using relative vorticity, whereas in analysis with ATAGC we use both relative vorticity and geopotential height anomaly for tracking LPS. Similarly, track density (number of tracks per year within 500 km of each grid location) obtained by applying ATAGC on ERA-Interim data and those from HB2015 are shown in Fig. 2c and d respectively. High values (around 12 tracks per year) are seen along the monsoon trough region indicating that most LPS form over northern BoB and move north westwards. The area integral for HB2015 is larger than that of ATAGC based on ERA-Interim data. This is not surprising, as the number of LPS and hence their genesis density and track density are larger for HB2015.

To identify the central domain of influence of the LPS, a median track is constructed. One way to construct a median track is to project the longitudes and latitudes of individual tracks onto a lifetime axis (0.0 at genesis, 1.0 at lysis, 0.5 for the timestamp equidistant from lysis and genesis) and then take the mean of longitudes and latitudes corresponding to the different points on the lifetime axis. On a lifetime axis, the median track of HB2015 and ATAGC based analysis is as shown in Fig S5. As both genesis and lysis span almost 40 degrees along longitude (60E–100E), the median track is found to be very short. Hence an alternate method is adopted to determine the location of median track. A longitudinal belt extending from 76° E to 90° E is considered, as it encompasses the genesis and tracks of most LPS. The belt is divided into longitudinal sections of width 1° each, and the median latitudinal location of tracks in each section is determined. The median track is obtained by joining the median latitudinal track locations of each longitudinal section. The median track obtained from our analysis and that constructed for tracks of HB2015 are shown in Fig. 3a. In both the cases, the median track forms over northern BoB and moves north-westwards. However, a small latitudinal shift to the north (by less than 1°) is found in our analysis compared to the median track of HB2015. This is because a

Fig. 2 LPS genesis density (number of genesis locations per year within 500 km radius of the location) identified by analyzing **a** ERA-Interim data using the tracking algorithm ATAGC for the period 1979–2015 and **b** those in HB2015 for the period 1979–2012. LPS tracks density (number of tracks per year passing within 500 km radius of the location) during the same period **c** from ERA-Interim data using ATAGC and **d** in HB2015. The LPS mostly form on northern BoB and move north westwards. **b**, **d** shows tracks from HB2015 which have at least one track location in the area of our study



large number of tracks are identified in the southern peninsular region in HB2015 (Fig. 2c, d). This can be attributed to the difference in the method of identification of LPS: our algorithm tracks LPS using both vorticity and 850 hPa geopotential criteria, while LPS in HB2015 is tracked using only relative vorticity maxima, though categorization is based on sea level pressure anomaly and maximum wind speed along the track. As vorticity anomalies appear earlier in time compared to pressure anomalies (Hurley and Boos 2015) it is likely that our algorithm does not identify the much weaker LPS in the southern peninsula leading to a slight northward shift in median tracks in our analysis. The difference in number of LPS genesis locations per year obtained based on analysis with ATAGC and HB2015 is more pronounced over ocean than land. Over land, the numbers are 7.18 and 7.44 in analysis based on ATAGC and HB2015 respectively. Whereas, over oceans, the corresponding numbers are 5.67 and 8.14 respectively. However, the main area affected by LPS remains the same in both analyses, i.e., east and central India (Fig. 3a).

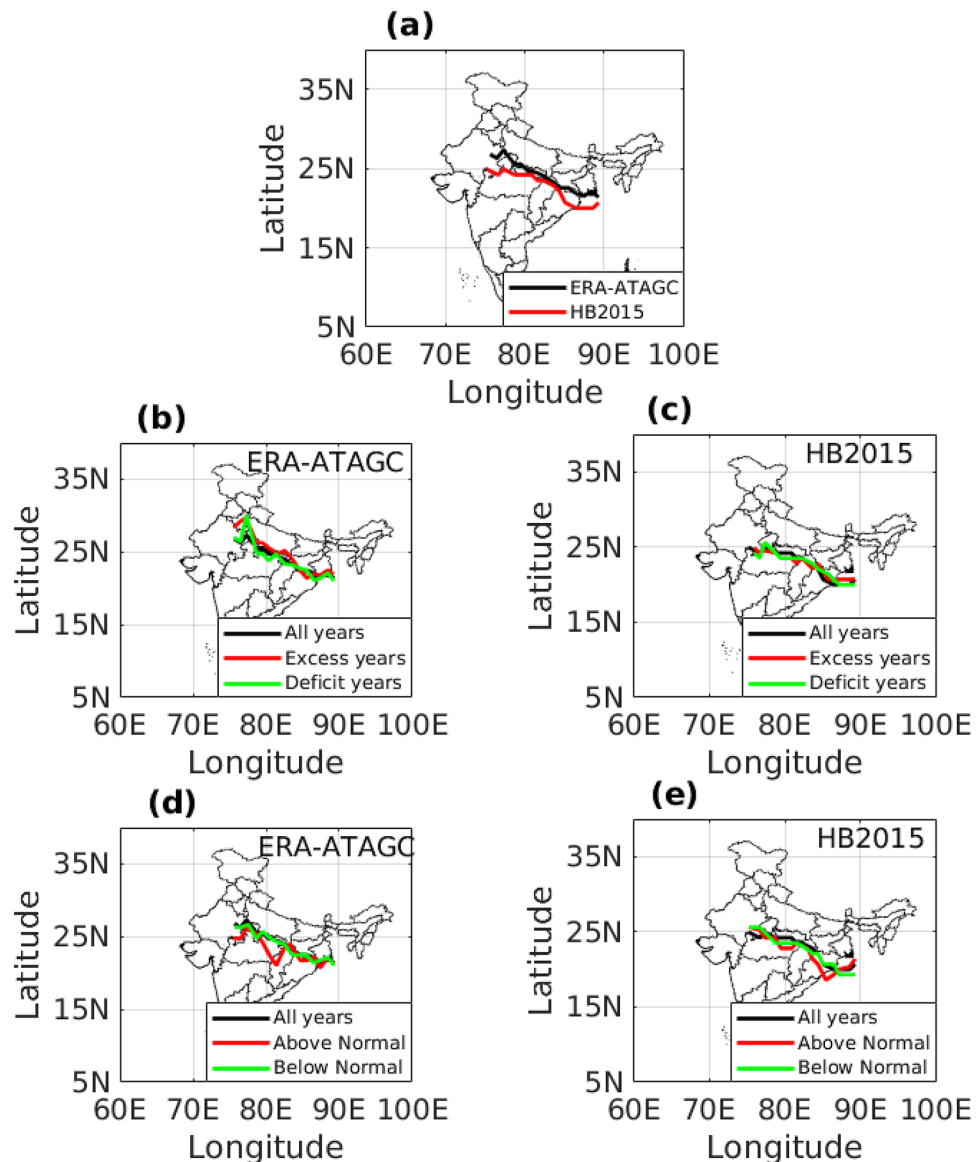
IMD classifies a year as an excess (deficit) rainfall year if monsoon (JJAS) seasonal mean precipitation anomaly is larger (lesser) than 10% of mean Indian summer monsoon

precipitation (ISMR). During the period 1979–2015, the number of excess and deficit precipitation years are counted as 3 and 10 years respectively by IMD. Three median tracks of LPS are constructed, first one using LPS tracks of excess years, the second one using LPS tracks of deficit years, and the third one constructed using LPS tracks of all the years (Fig. 3b, c). The median tracks obtained from our analysis with ATAGC (Fig. 3b) are compared with those from HB2015 (Fig. 3c). In the case of ATAGC, the median track for excess (deficit) precipitation years is found to be marginally shifted towards north (south) of the median track of all years. The shift is however not significant. In the case of HB2015, the median tracks corresponding to excess and deficit years do not indicate any shift. When the precipitation in a year is 106–110% (90–96%) of the mean ISMR, the year is considered as above (below) normal precipitation year. During the period 1979–2015, three above normal precipitation years and six below normal precipitation years are identified in our analysis with IMD precipitation data. The median LPS track corresponding to the above normal precipitation years appears marginally shifted southward compared to median track of all years over most of the

Fig. 3 Median LPS track obtained in analysis with **a** ERA-Interim data using the ATAGC algorithm for the period 1979–2015 and HB2015 for the period 1979–2012.

The median track is obtained by connecting the median locations of tracks observed in 1° longitudinal belts between 75°E – 90°E . Median tracks obtained for excess and deficit years using **b** ATAGC algorithm and **c** HB2015.

Median tracks for above normal precipitation years and below normal precipitation years in analysis with **d** ERA-Interim data using ATAGC algorithm and **e** HB2015. Excess (deficit) years are those with precipitation anomaly greater (less) than 10% of mean Indian summer monsoon precipitation (ISMR). Above (below) normal precipitation years are those with precipitation anomaly greater (less) than 5% of ISMR



longitudinal range in analysis based on tracks of ATAGC and HB2015 (Fig. 3d, e).

Krishnamurthy and Ajayamohan (2010) estimate 13 excess precipitation years and 20 deficit precipitation years during 1901–2003. During that period on an average around 2 more LPS and 10 more LPS days are estimated in excess years as compared to deficit years. Our analysis over the period 1979–2015 indicates 5 more LPS (comprising 4 lows and 1 depression) and 15 more LPS days during excess precipitation years compared to deficit years (Table 2). In addition, 1.5 more LPS and 5 more LPS days are estimated for above normal precipitation years compared to below normal precipitation years. The larger difference in number of LPS and LPS days between excess and deficit years in our analysis compared to earlier studies is attributable to difference in study duration (time window) considered in the analysis.

But the general trend of higher number of LPS and LPS days during excess years compared to deficit years is consistent in our analysis too. The correlation between the annual precipitation anomaly and the number of LPS is estimated as 0.45 (Fig. S6), indicating that the number LPS has an influence on the annual summer monsoon precipitation over India, but it is not the sole factor controlling the precipitation.

4.2 Interannual variability in number of LPS and LPS days

As discussed earlier, LPS are classified as lows, depressions and deep depressions based on various criteria (Table 1). Table 1a shows the criteria used for classifying tracks of HB2015 and Sikka archive, whereas Table 1b shows the criterion used by ATAGC for application on ERA-Interim

Table 2 Average number of different categories of LPS and LPS days per year during normal (96–104 % of mean ISMR), excess (>110%), deficit (<90 %) above normal (104–110) and below normal (90–96) years during the period 1979–2015

	No. of years	Total LPS	Lows	Depressions	Deep depressions	Depressions + deep depressions	LPS days
Excess rainfall years	3	17.0	11.0	6.0	0.0	6.0	75.3
Above normal years	3	14.7	9.0	5.3	0.3	5.7	73.0
Normal monsoon years	15	15.1	9.0	5.9	0.1	6.1	72.1
All years	37	14.1	8.8	5.1	0.2	5.3	68.0
Below normal years	6	13.2	9.8	3.2	0.2	3.3	68.0
Deficit years	10	12.0	7.2	4.5	0.3	4.8	59.8
Highest rainfall year (1988)	1	18	12	6	0	6	68
Lowest rainfall year (2002)	1	12	7	5	0	5	61

reanalysis data product. Since surface roughness lengths vary significantly with model resolution in reanalysis datasets and have a strong effect on surface winds, we use 850 hPa wind instead of surface winds as in Hunt et al. (2017) for categorizing of LPS. For the time period 1979–2003, Sikka's archive shows around 14 LPS per year comprising 10 lows, 2.5 depressions and 1.5 deep depressions (Hurley and Boos 2015). For the same period, HB2015 estimates around 16 LPS per year which consist of about 12 lows, 4 depressions and less than one deep depression. Our analysis shows around 14 LPS per year comprising 9 lows, 5 depressions and less than 1 deep depression a year. Interannual variability of the number of systems determined using different algorithms is shown in Fig. 4. It can be noted from

the figure that ATAGC yields similar mean number of LPS per year as in Sikka's and IMD archives, whereas HB2015 has a larger number of LPS per year. Further, LPS annual frequency discerned from our analysis has low, but statistically significant correlation of 0.34 (at 5% significance level) with annual frequency from Sikka's archive. Correlations of annual counts of lows, depressions, and sum of depressions and deep depressions from ATAGC tracks with the corresponding counts from Sikka's archive are found to be 0.23, –0.06 and 0.07 respectively. In contrast, estimates of the same between HB2015 and Sikka's archive are all found to be negative (–0.34, –0.29 and –0.17 respectively). Estimates of the correlations between ATAGC tracks and HB2015 are also low (0.06, 0.39 and 0.5 respectively). These

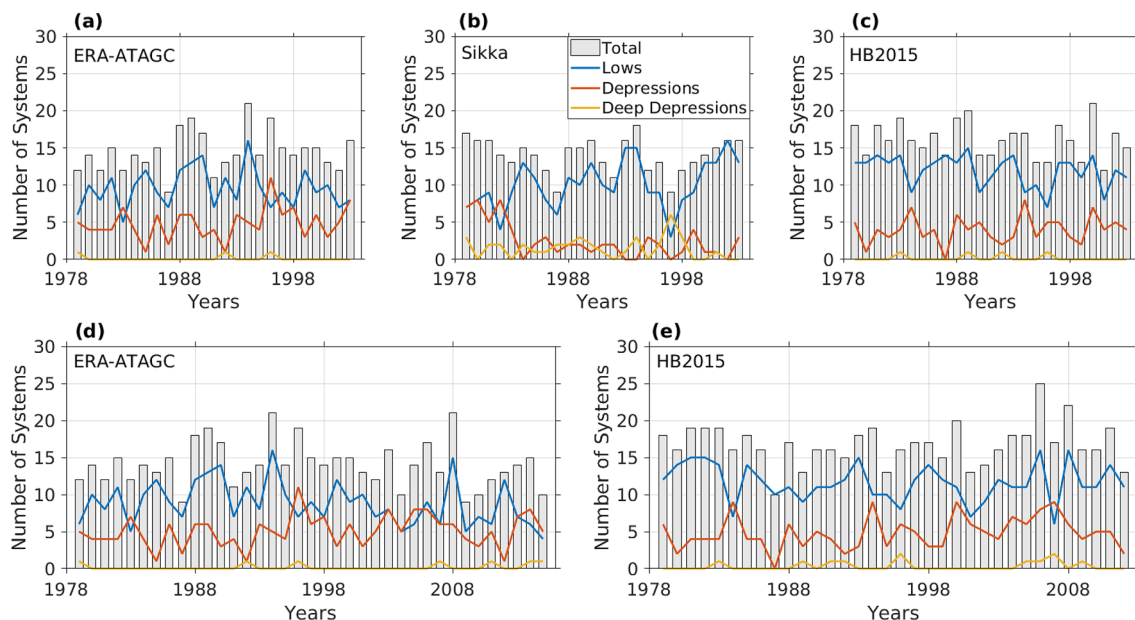


Fig. 4 Time series of annual number of different categories of LPS for the period 1979–2003 in **a** our analysis with ATAGC on ERA-Interim data product, **b** Sikka archive and **c** HB2015. The same

is shown for **d** the period 1979–2015 in our analysis with ATAGC applied on ERA-Interim and **e** the period 1979–2012 in HB2015

low correlations indicate very little agreement in the number of various categories of LPS tracked by the ATAGC and previous studies on a year-to-year basis. This is likely due to the subjectivity involved in the identification of genesis points and tracking of LPS as discussed in the Introduction section. However, there is some resemblance in the general pattern of genesis and track locations (Fig. 2) between our analysis and HB2015.

Earlier studies on Sikka archive revealed a significant decreasing trend in the number of depressions (Sikka 2006; Patwardhan and Bhalme 2001; Mandke and Bhide 2003), though there is significant increase in extreme precipitation events. Later, Ajayamohan et al. (2010) analyzed the same data and found a significant increase in lows, which have contributed to the increase in extreme precipitation. In a related study (Cohen and Boos 2014), which generated HB2015 using ERA reanalysis data products, no such decrease was found in the number of depressions. Analysis of the dataset for the period 1979–2003 revealed a non-significant increasing trend in the number of depressions, and non-significant decreasing trend in the annual number of LPS and lows. In analysis with ATAGC based tracks obtained in the current study, non-significant decreasing trend in the number of LPS and lows, and non-significant increase in depressions is found when examined using Mann–Kendall test considering 95% confidence level. These results are consistent with those of Cohen and Boos (2014) based on HB2015. In a recent study that considered multiple reanalysis data products, long-term reduction in depressions was not observed. Trend was observed in some LPS datasets, which was attributed to change in observation network with introduction of geostationary satellite data (Vishnu et al. 2020).

For the period 1979–2003, Sikka's archive shows maximum LPS activity in the month of August followed by July (Fig. S7) when most LPS form by downstream amplification of wave disturbances from western Pacific (Meera et al. 2019). However, maximum LPS activity occurs in the month of July followed by June in HB2015, and some of those LPS may be heat induced lows over the desert region (Fig. S4(c)). Similar to Sikka's archive, ATAGC applied on ERA-Interim data also shows the largest LPS activity in the month of August followed by July (Fig. S7). The monthly average number of lows in our analysis (1.5 in June, 2.6 in July, 3.0 in August and 2.4 in September) is comparable to that of Sikka's archive (1.8, 2.8, 2.8, 2.6), but the number of depressions in our analysis (1.84, 1.4, 1.12, 0.48) is slightly larger when compared to that in Sikka's archive (0.63, 0.43, 0.86, 0.43) especially in the months of June and July. Even though Sikka's archive has larger number of deep depressions compared to ATAGC, the monthly average frequency of stronger systems (depressions + deep depressions) is still larger in

case of ATAGC (1.92, 1.4, 1.12, 0.52) compared to Sikka's archive (1.18, 0.59, 1.29, 0.79). This is likely attributable to the subjectivity involved in tracking of these LPS. The use of 850 mb wind instead of surface winds in our tracking scheme is also a likely cause. While keeping the wind speed thresholds same for categorizing of systems, we have used the more steady and much stronger 850 hPa wind, whereas Sikka has used surface wind fields.

Out of the 122 days of monsoon period (June–September), LPS are present in the study area for about 59 days in Sikka's archive (Praveen et al. 2015), and for around 90 days in HB2015 dataset. The corresponding number is found to be 68 days in our analysis. The interannual variability of the frequency of LPS days estimated by different methods is shown in Fig. 5. The Pearson's product moment correlation between annual frequency of LPS days based on Sikka's and ATAGC tracks is 0.45, whereas that between Sikka's and HB2015 tracks is 0.38, while the same between HB2015 and ATAGC tracks is 0.45. The low values of correlation can be attributed to the subjectivity involved in the algorithms used for identification of LPS tracks.

Contrary to the expectation that number of LPS and hence number of LPS days would be related to large scale interannual variability of recurring climate patterns such as ENSO, the number of LPS days in a monsoon season has been found to be associated with small scale features such as strength and location of monsoon trough and number of active and break days during monsoon (Sikka 1980). During the period 1888–2003, the number of LPS days and the location and spatial extent of LPS were found to be nearly equal in both El-Niño and La-Niña years (Krishnamurthy and Ajayamohan 2010). In that study, estimate of correlation between the number of LPS days and JJAS Niño3.4 index was found to be -0.07. The corresponding estimate obtained in the present study with ATAGC is also low (-0.12) for the period 1979–2015 (Fig. 5b). While analyzing the correlation of total number of LPS, lows and depressions plus deep depressions with Niño3.4 index, small yet negative correlations (-0.25, -0.18, -0.09) are obtained for the aforementioned study period. The consistency in the sign of the correlation indicates that the LPS activity is slightly reduced during El Nino years but the small magnitude indicates that ENSO variability is likely to explain only a small component of the interannual variability in LPS activity. Indian Ocean Dipole (IOD), the dominant interannual variability in the Indian Ocean basin, is shown to have less influence than ENSO on monsoon depressions (Hunt et al. 2016). However, IOD is found to have an influence on the lifetime of LPS (Krishnan et al. 2011). It is likely that ENSO, IOD and other large scale interannual variations in Atlantic sea surface temperature and Eurasian snow cover may have indirect effect on LPS by affecting the strength of the monsoon trough and active-break phase cycle during monsoon. Further research

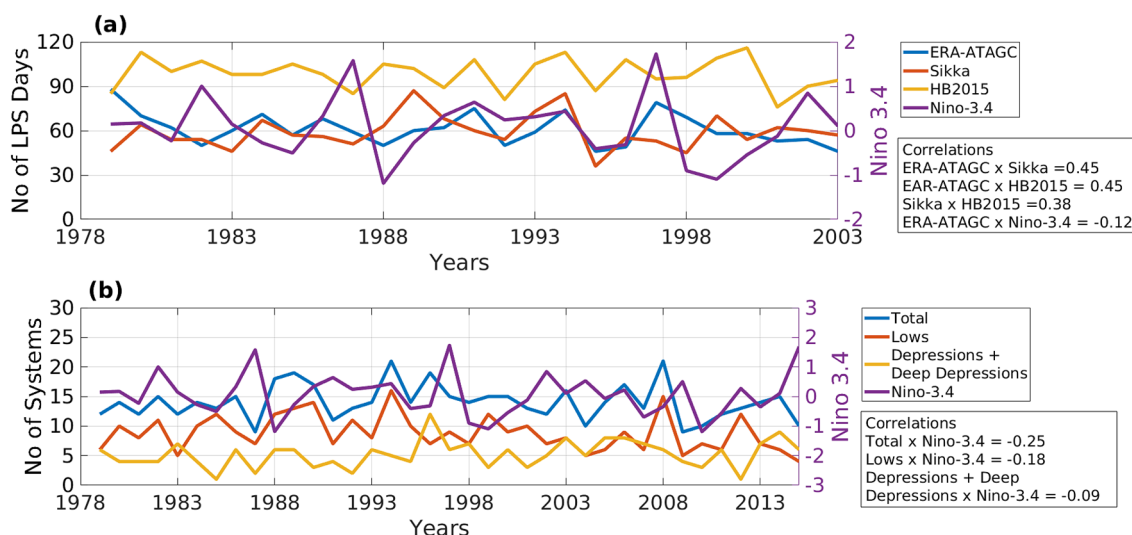


Fig. 5 **a** Number of LPS days in each year and Nino 3.4 index during the period 1979–2003. LPS days are the days on which an LPS is present in the study area. LPS days determined from Sikka archive (Praveen et al. 2015) are compared with those obtained by analyzing

data from HB2015 and in our analysis using ATAGC on ERA-Interim data. **b** Number of different categories of LPS and Nino 3.4 index during the period 1979–2015. Correlation between number of different categories of systems and Nino 3.4 index is found to be negative

is needed to investigate the mechanisms that drive the interannual variability in LPS statistics.

4.3 Comparison of tracks

Probability of coincidence is a measure which quantifies the percentage of identical tracks (i.e., tracks similar to each other in space-time domain) between given two sets of tracks. The term “identical tracks” does not mean an exact match from genesis to lysis, but it refers to tracks that are most near to each other in space-time domain when compared to all other tracks. It can be determined using Blender and Schubert algorithm (Blender and Schubert 2000), which is described in the Supplementary material (Section S2.1). For each year, the probability of coincidence of ATAGC based LPS tracks with IMD archive and HB2015 based tracks was determined (Fig. 6). The ATAGC based tracks have 100% probability of coincidence with IMD tracks for the period 1989–2003, indicating that all the depressions and deep depressions in IMD archive during the period have been identified by ATAGC, except for a system that formed over Arabian sea in 1998 and another system over land in 1996, which lasted in the study area for less than 2 days. Since our algorithm identifies systems with a lifetime of more than 2 days in the study area, these two systems tracked by IMD are not identified. The probability of coincidence between ATAGC and HB2015 based tracks is greater than 50% for all the years (except 1996), which is deemed fairly high. Similar analysis in a recent study (Praveen et al. 2015), indicated probability of coincidence values in the range 7–53% between tracks obtained in Sikka archive and those

obtained by automated tracking of LPS considering ERA-Interim reanalysis and MERRA reanalysis data products.

IMD publishes details of the monsoon activity over Indian subcontinent in its yearly report called Mausam (IITM 2015; IMD 2011, 2012, 2013, 2014, 2015). The report provides a map of the tracks of depressions and deep depressions along with an overall number of LPS that form each year during the summer monsoon time, but it does not provide the tracks of lows. A comparison of the number and the category of LPS observed by IMD and that obtained by applying ATAGC on ERA-Interim data is provided in Table S2. The tracks of the six depressions and deep depressions that are observed by IMD (IITM 2015) and also tracked by ATAGC on ERA-Interim dataset for the year 2015 are shown in Fig. S8. For the year 2014, IMD has identified 13 LPS, among which there are 2 depressions, 1 deep depression and 10 lows (IMD 2015). The tracks of these depressions and deep depressions that are observed by IMD and also tracked by ATAGC based on ERA-Interim dataset are shown in Fig. S9. The deep depression observed during 10–14 June 2014 over the Arabian sea is identified as a tropical cyclone. It is the only tropical cyclone identified using the criteria discussed in Sect. 2. This cyclone, which is named NANAUK (IMD 2015), is not included in our analysis of monsoon LPS. For the year 2013, 18 LPS including 2 depressions have been reported by IMD (IMD 2014). The tracks of these two depressions that are observed by IMD and also tracked by ATAGC based on ERA-Interim dataset are shown in Fig. S10. IMD does not identify any depression in the year 2012, but ATAGC finds one depression and HB2015 identifies 2 depressions in that year. Agreement in the spatial pattern of

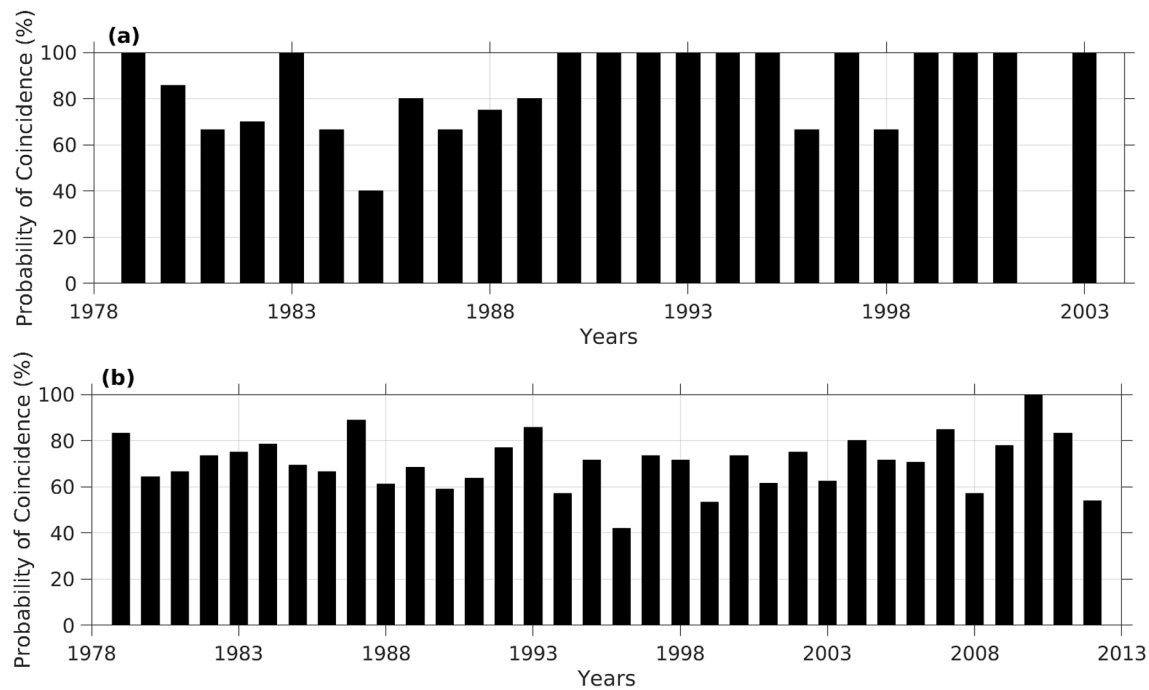


Fig. 6 Probability of coincidence between **a** ATAGC and IMD tracks and during the period 1979–2003 **b** ATAGC and HB2015 tracks during the period 1979–2012, estimated using Blender and Schubert algorithm

LPS tracks between our analysis and IMD (Figs. S8–S10) gives confidence in using our algorithm for further analysis.

4.4 Precipitation associated with LPS

Precipitation composite (i.e., average daily precipitation) on LPS days is estimated for the monsoon period using IMD daily precipitation data ($0.25^\circ \times 0.25^\circ$). The spatial patterns of precipitation composite corresponding to tracks in HB2015 and ATAGC are shown in Fig. 7, which appear quite similar (with a correlation coefficient 0.99) and comparable to that estimated using Sikka's archive (Fig. 3a, Krishnamurthy and Ajayamohan 2010). The Root Mean Squared Difference (RMSD; Section S2.2), between estimates of precipitation composite corresponding to ATAGC and HB2015 tracks is found to be 1.3 mm/day. Mean of precipitation composite based on HB2015 tracks is 7.2 mm/day and that for ATAGC based tracks is 7.96 mm/day, and hence the RMSD is small (<20% of the mean). The lower mean value in case of HB2015 dataset is likely due to larger number of weaker LPS (Fig. 4). Larger precipitation on LPS days is found in the Central Indian states namely Odisha, Chhattisgarh and Madhya Pradesh (Fig. S11) and along the Western Ghats. In analysis with ATAGC based tracks, precipitation on LPS days is found to be 70–80% of monsoon precipitation over the core monsoon region and along Western Ghats (Fig. 7c). However, in analysis with HB2015 based tracks, the corresponding percentage is found to be relative higher

(around 70–90%) over the whole country, except the dry interior regions of south India (Fig. 7d). This is not surprising because the average number of LPS days is much higher (90 days) in the case of HB2015 when compared to that (68 days) in case of ATAGC based tracks.

Daily mean precipitation at locations at a distance less than or equal to 1000 km from LPS track is estimated on LPS days. This may be considered as the precipitation associated with LPS tracks. Spatial pattern of such estimates corresponding to HB2015 and ATAGC based tracks appears similar (Fig. 8) and the correlation between these estimates (=0.98) is found to be statistically significant at 98.9% confidence level when tested using Fisher z-transformation test. Further, RMSD between estimates corresponding to the HB2015 and ATAGC tracks is 2.97 mm/day. The estimates of spatial average precipitation are found to be 14.04 mm/day and 12.97 mm/day respectively for ATAGC and HB2015 based tracks. Hence, the RMSD is small (~23% of the mean). The spatial pattern in Fig. 8 shows clearly that precipitation in east and central India are strongly associated with LPS. The average daily monsoon rainfall in east and central India is also high compared to other parts of the country (Fig. S12a). This emphasizes the fact that, monsoon brings copious rain to the above-mentioned regions and most of it is associated with LPS. 60–70% of monsoon precipitation in north Indian region is also found to be associated with LPS (within 1000 km radius of LPS; Fig. S12c). Even though LPS associated precipitation is large on the

Fig. 7 Precipitation composite (i.e., average daily precipitation (in mm/day)) on LPS days based on **a** ATAGC during the period 1979–2015 and **b** HB2015 during the period 1979–2012. Percentage of precipitation occurring on LPS days to total precipitation based on **c** ATAGC during the period 1979–2015 and **d** HB2015 during the period 1979–2012. The median tracks (black solid lines) corresponding to ATAGC and HB2015 are shown. For estimation of the composite precipitation, IMD daily precipitation data are used ($0.25^\circ \times 0.25^\circ$ resolution)

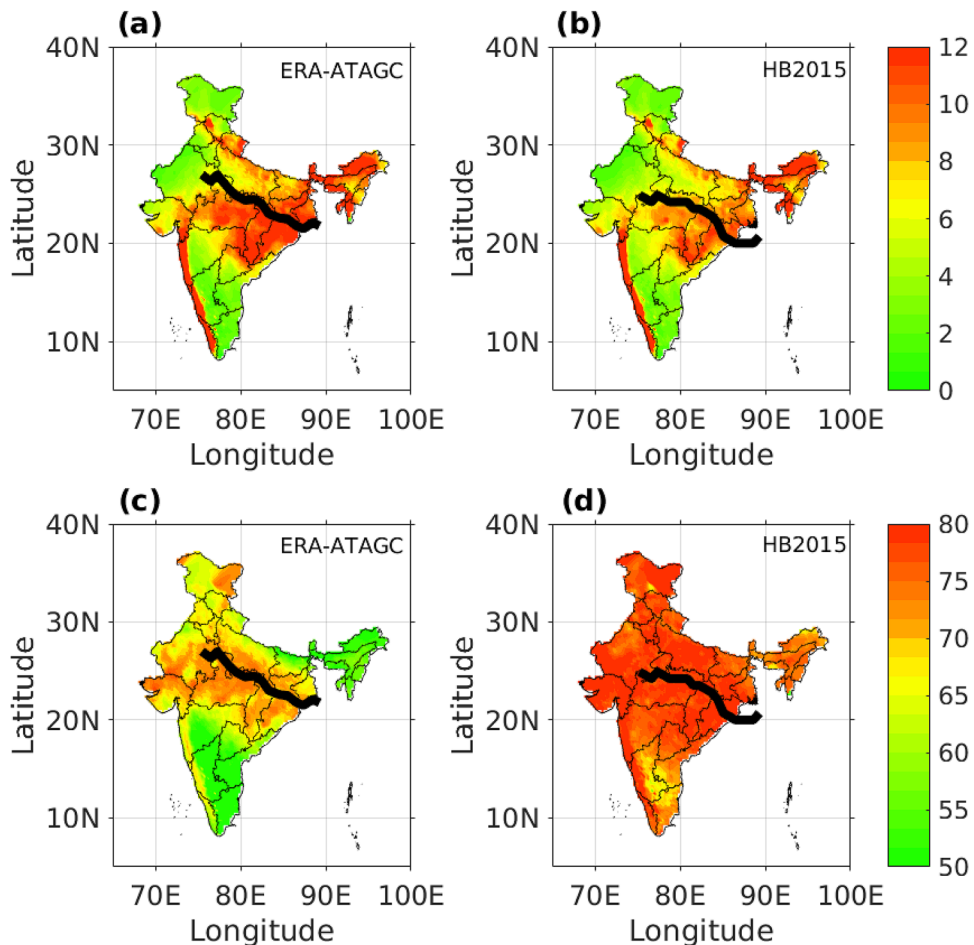
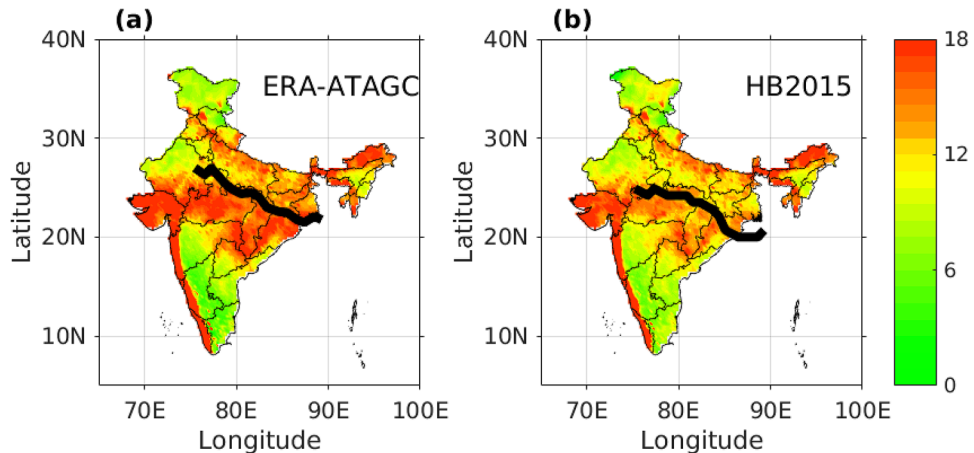


Fig. 8 Average daily precipitation (in mm/day) within 1000 km radii of tracks based on **a** ATAGC during the period 1979–2015, **b** HB2015 during the period 1979–2012. The median tracks (black solid lines) corresponding to ATAGC and HB2015 are shown. Estimates are based on daily precipitation data obtained from IMD ($0.25^\circ \times 0.25^\circ$ resolution) during the same period



south side of the median track (Fig. 7), the contribution of LPS related precipitation to total monsoon precipitation (in percentage) is similar on both north and south of the median tracks. The larger values in the west coast of India are likely associated with the few LPS that originate below 20°N (Fig. S4(b)). Though such systems are few in number, other factors like orographic uplift and water vapor supply

are much favorable to cause high rainfall events in the region of western Ghats.

Previous studies (Hunt and Fletcher 2019) have analyzed the sensitivity of using a fixed radius (800 km) approach for determination of precipitation associated with LPS in the Indian subcontinent. Throughout our analysis we have attributed precipitation around 1000 km radii of LPS track

to be associated with LPS. To analyze the sensitivity of average daily precipitation estimate associated with LPS on the radius chosen (1000 km), the analysis was repeated by using 500 km and 800 km radii. The results (Fig. S13) indicate that spatial pattern of the average precipitation (corresponding to the three different radii) are quite similar. Correlation between the spatial pattern of precipitation corresponding to 500 and 1000 km radii criteria is 0.96, whereas that between 800 and 1000 km radii criteria is 0.99. Further, RMSD between precipitation estimates corresponding to 500 and 1000 km radii criteria is 8.08 mm/day, whereas that between estimates corresponding to 800 and 1000 km radii criteria is relatively less (2.25 mm/day). The estimates of spatial average precipitation corresponding to 1000, 800 and 500 km radii are 14.04 mm/day, 15.34 mm/day and 19.5 mm/day respectively. Even-though the average precipitation estimates vary for different radii of influence, the large value of correlation coefficient found in our analysis corresponding to 1000 km and 800 km radii (used by Hunt and Fletcher 2019) and smaller RMSD between precipitation estimates corresponding to these two cases provides confidence to using 1000 km as radius of influence for further analysis.

4.5 Synoptic activity index

Synoptic activity Index is a metric useful to identify the LPS activity at a location in terms of both intensity and number of systems (Ajayamohan et al. 2010). The number(count) of different categories of LPS (i.e., lows, depressions, deep depressions) which originate or traverse through each location is obtained and the weighted sum of the counts over the period 1979–2012 is estimated as SAI for the location. The weight depends on the category of the system. The weight for each category of the LPS is taken as the centroid of the wind speed range of that particular category of LPS as shown in Table S1. A detailed description of the procedure for estimating SAI is provided in the Supplementary

material (Section S3). The SAI for ATAGC and HB2015 based tracks, estimated on a $3^\circ \times 3^\circ$ grid, is shown in Fig. 9. The spatial correlation between SAI estimates is around 0.76. It can be noted from Figs. 9a, b that SAI is larger near northern Bay of Bengal (where LPS generally originate) and its value remains large towards north-west direction in which LPS generally propagate. The largest values of SAI are an indication that the area is strongly affected by these LPS. The trend in annual estimates of SAI is determined for each location using Mann–Kendall test by considering 95% confidence level. Estimates of the test statistic obtained in analysis with ATAGC (1979–2015) and HB2015 (1979–2012) based tracks are shown in Fig. S14. The results indicate that trend in SAI is generally not significant. The trend is positive for locations having large values of SAI, but the positive trend is mostly not significant.

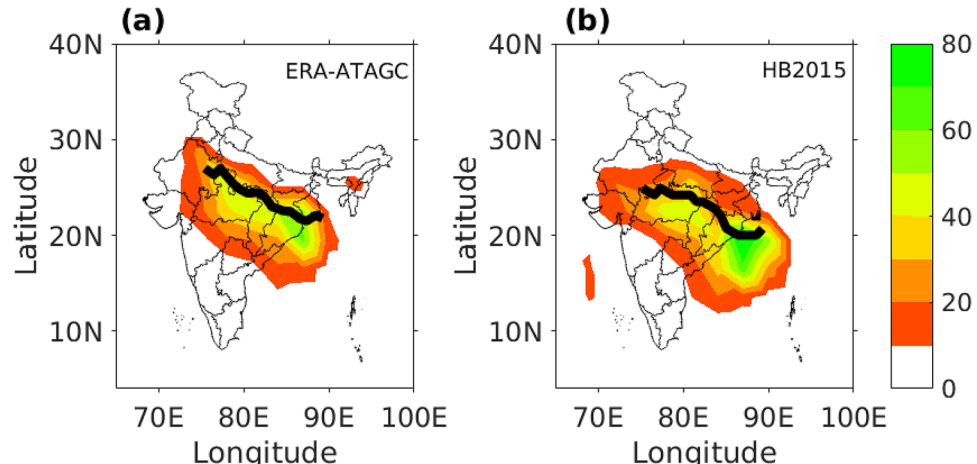
Monsoon LPS are not as intense as tropical cyclones, and hence their effect is not in the form of maximum wind, but in the form of extreme precipitation around LPS. Therefore, SAI which accounts for wind speed and number of systems may not be an effective indicator of the damage caused by extreme precipitation in the country. A flood-risk map for the country associated with LPS related extreme precipitation events can be used as a valuable tool in assessment of flood risk in the monsoon period.

As the known statistical features of the LPS (from literature) are confirmed for the tracks obtained using ATAGC, they are used for further analysis to estimate LPS related extreme precipitation statistics in India.

4.6 Extreme precipitation analysis

For extreme precipitation analysis, 0.25° resolution IMD gridded daily precipitation data are considered. If precipitation at a location is greater than 64.5 mm/day, IMD classifies it as heavy precipitation event. Hence, in our analysis, if the daily precipitation at any location within 1000 km of LPS

Fig. 9 Synoptic activity index (SAI) estimated for **a** ATAGC during the period 1979–2015, and **b** HB2015 based LPS tracks during the period 1979–2012. The median tracks (black solid lines) corresponding to ATAGC and HB2015 are also shown. Procedure for the estimation of SAI is discussed in supplementary material (section S3)



track is greater than 64.5 mm, it is classified as LPS related extreme precipitation event.

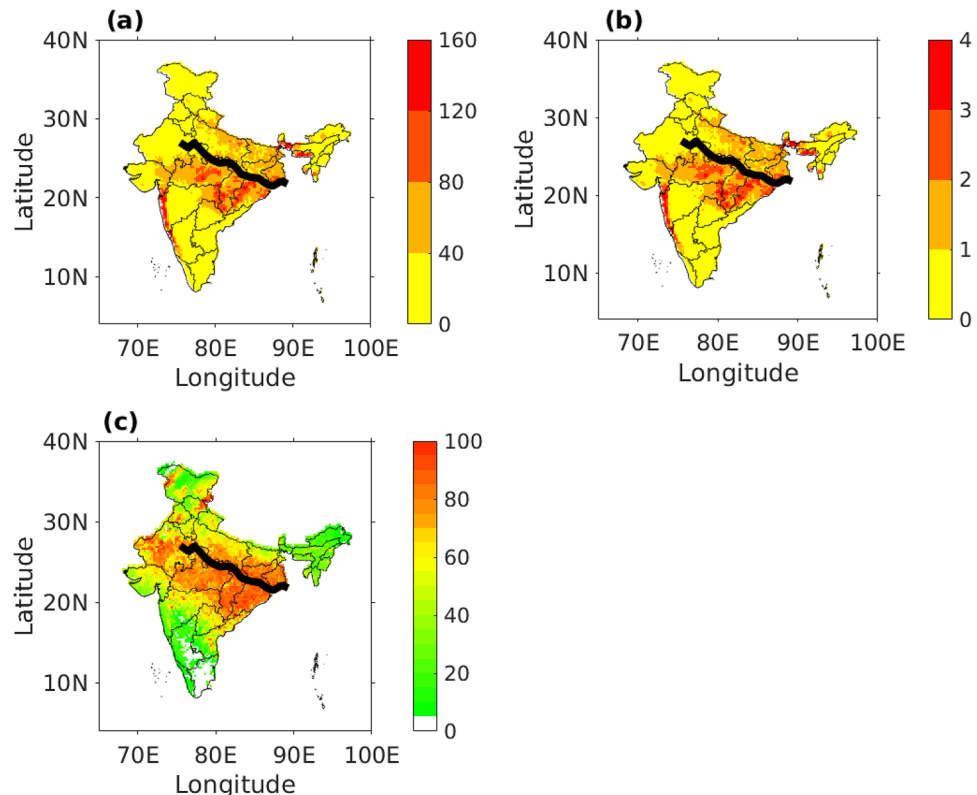
Figure S15 shows the spatial variability of frequency/number of extreme events based on IMD (1979–2015) and TRMM (1989–2015) gridded ($0.25^\circ \times 0.25^\circ$) data. Correlation of the frequency estimates based on IMD and TRMM data is fairly large (0.87). Since IMD data are available for the entire study period (1979–2015), extreme precipitation analysis is performed using IMD data. The frequency estimates are larger in central part of India during the summer monsoon season and most of the extreme precipitation events are found to occur during the LPS days, as found by Krishnamurthy and Ajayamohan (2010).

Frequency of extreme precipitation events within 1000 km radius of LPS are analyzed (Fig. 10a). We find a large number of extreme events on the south side of the median LPS track. This is consistent with earlier studies (Sikka 2006; Krishnamurthy and Ajayamohan 2010; Hunt et al. 2016) which show that the maximum precipitation is located on the south-west quadrant of LPS. The extreme events which occur in north-east India are likely influenced by orography of the Himalayas apart from LPS. But the extreme events in central India are likely a manifestation of LPS. The frequency/number of extreme events in central India (covering Madhya Pradesh, Chhattisgarh and Odisha states; see Fig. S11) varies in the range 40 to 120 during 1979–2015, which is relatively larger than that

noted for rest of the country. This could be attributed to the fact that the locations in central India are more prone to LPS related extremes. Figure 10b shows the average number of extreme events per year associated with LPS. Many locations in the central Indian region experience 2–4 LPS related extreme events per year. Previous studies (e.g., Goswami et al. 2006) have found an increasing trend in the frequency of extreme precipitation events (> 100 mm/day) in the central Indian region ($18.5\text{--}26.5^\circ\text{N}$, $77.5\text{--}86.5^\circ\text{E}$) with analysis using IMD precipitation data ($1^\circ \times 1^\circ$) for the period 1950–2000. Since our study period is too short (37 years), we do not perform a trend analysis here to determine any change in number of extreme events associated with LPS.

Ajayamohan et al. (2010), while analyzing IMD precipitation data ($1^\circ \times 1^\circ$) for the period 1951–2003 over central Indian region ($18.5\text{--}26.5^\circ\text{N}$, $77.5\text{--}86.5^\circ\text{E}$), found that 62% of extreme precipitation events are LPS related. In that study, daily precipitation at any location within 5° radius of the LPS track and exceeding 98.3rd percentile of precipitation observations at that location is considered as LPS related extreme precipitation event. In our analysis, which covers 1000 km around LPS over the same region, 78% of extreme precipitation events (having daily precipitation greater than 64.5 mm) are found to be associated with LPS. We find that over the same region 82% of extreme events occur during LPS days, out of which 47% are on depression and deep

Fig. 10 Extreme events (daily precipitation greater than 64.5 mm) at grid points/locations within 1000 km radii of ATAGC based LPS tracks during the period 1979–2015: **a** total count (frequency), **b** annual frequency, and **c** ratio (in %) of number of LPS-related extremes to the total number of extremes during monsoon over the period 1979–2015. More than 80 percent of the extremes observed at locations in central India occur when a LPS passes within 1000 km radii of the locations. Median track (black solid line) obtained using ATAGC based LPS tracks is also shown



depression days. Most extremes (> 80%) in central and east Indian states are associated with LPS (Fig. 10c).

In the study period (1979–2015), 4724 grids/locations (on the grid with a resolution of $0.25^\circ \times 0.25^\circ$) covering 27% area of the Indian mainland have experienced at least one extreme precipitation event due to LPS. In the first decade (1979–1989), around 3825 locations (22% area of the country) witnessed extreme events due to LPS with an average of around 12 extreme events per location, while in the second decade (1990–2000), around 4489 locations (25% area of the country) experienced extreme events due to LPS with around 11.8 extreme events per location. In the last decade (2001–2011), a comparable number (4040) of locations (23% area of the country) are affected by the extreme events due to LPS, with around 12 extreme events per location.

The spatial pattern for ratio of LPS related extreme precipitation to the total precipitation (Fig. 11) is found to be very similar to Fig. 10c. Around 15–25% of monsoon precipitation in east, central and west Indian regions can be attributed to extreme storms caused by LPS. Many locations in Madhya Pradesh, Chhattisgarh, Gujarat and Odisha and coastal locations of Maharashtra (Fig. S11) receive majority of their precipitation in the form of extreme storms when an LPS passes nearby. In east and central Indian regions, the locations corresponding to large values of the ratio appear to coincide with the locations for which total count (frequency) of the extreme precipitation events associated with LPS is larger (Fig. 10a). However, the percentage of total

extreme precipitation events associated with LPS (Fig. 10c) and the percentage of extreme precipitation contributed by those events (Fig. 11) is less than 10% along the coastline of western Ghats, even though number of LPS related extreme events (Fig. 10a), precipitation occurring on LPS days (Fig. 7) and average precipitation contributed by LPS within 1000 km radii of a grid (Fig. 8) is large along the west coast. This is not surprising because west coast of India receives high precipitation and experiences large number of extremes not only due to LPS, but also due to other factors such as orography and water vapor supply from the adjoining ocean. Hence, when percentage of extreme rainfall events related to LPS (Fig. 10c) and percentage of extreme rainfall related to LPS (Fig. 11) are calculated, smaller values are obtained for grids along the west coast.

IMD classifies a precipitation event as very heavy, if daily precipitation is greater than 124.5 mm/day. At each location, extreme precipitation events during LPS days and within 1000 km radius of LPS tracks are determined for each year during the period 1979–2015. Precipitation corresponding to the events in each year are sorted to identify the largest value, which is referred to as the annual maximum extreme precipitation associated with LPS at the location for the chosen year. Frequency analysis is performed on annual maximum extreme precipitation values (corresponding to the period 1979–2015) for each location to determine the return period of very heavy precipitation events (events with precipitation greater than 124.5 mm/day) at that location. Similar to the above analysis of extremes due to LPS, many locations in central, west and east India show low values (1–5 years) of return period for very heavy precipitation (Fig. 12). The locations include Madhya Pradesh, Chhattisgarh, Gujarat and Odisha. Even though percentage of extreme precipitation associated with LPS is less along the western coast (Fig. 11), the number of extreme precipitation events due to LPS is high and comparable to those in the central India (Fig. 10a). Hence, return period of LPS related very heavy precipitation events along the west coast is comparable to that noted in central India (Fig. 12). Our analyses emphasize the fact that extremes due to LPS are a major source of monsoon precipitation in the country and also that east and central India are the major areas affected by extremes due to LPS.

The estimates of 99th and 95th percentile of extreme precipitation events obtained in analysis with (i) all extremes, (ii) extremes associated with LPS (when the grid location is within 1000 km of the track of a low pressure system), and (iii) extremes not associated with LPS (number of all extremes minus number of extremes associated with LPS) are shown in Fig. S16 for the study area. The 99th percentile here refers to the extreme precipitation that can be expected to occur at a location with a 1% chance. The estimates of extreme precipitation obtained

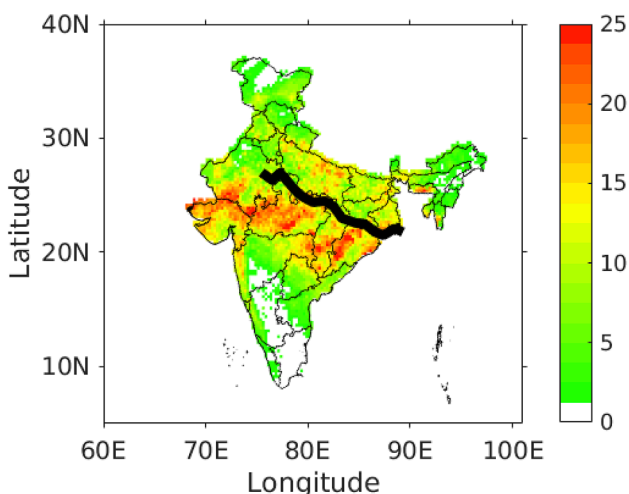


Fig. 11 Ratio (in %) of LPS-related extreme precipitation (within 1000 km of the centre of LPS) to the total precipitation observed during monsoon over the period 1979–2015 along with the ATAGC based median track (black solid line). The LPS tracks are obtained by applying ATAGC algorithm on ERA-Interim data, and IMD daily precipitation data ($0.25^\circ \times 0.25^\circ$ resolution) are used for extreme precipitation analysis. Around 15–25% of the total monsoon precipitation over east, central and west Indian regions is in the form of extremes that are associated with LPS

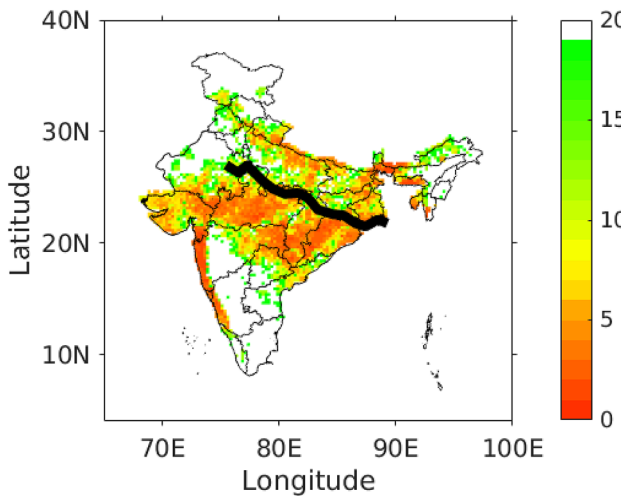


Fig. 12 Return period (in years) of very heavy rain (>124.5 mm/day) associated with LPS during the period 1979–2015. The gridded IMD precipitation data at a resolution of $0.25^\circ \times 0.25^\circ$ is used. To estimate return period for a location, frequency analysis is performed using annual maximum extreme precipitation values corresponding to LPS days when the location is within 1000 km radius of LPS tracks obtained by applying ATAGC algorithm on ERA-Interim data. The median track (black solid line) corresponding to ATAGC is also shown

using all extremes and those associated with LPS are very high at many locations in Madhya Pradesh, Chhattisgarh, Gujarat, and Odisha (Fig. S16 and S11). These locations receive heavy precipitation when a LPS passes nearby (Fig. S16(c), S16(d)) as compared to the case of no nearby LPS (Fig. S16(e), S16(f)). Over these states, the 99th percentile extreme precipitation varies from 200 to 300 mm in a day when LPS are present nearby, while it varies from 100 to 200 mm per day in the absence of a

nearby LPS. Similarly, the 95th percentile precipitation varies from 160 to 220 mm per day in the presence of nearby LPS, while it varies from 100 to 160 mm per day in the absence of nearby LPS. Hence, our analysis shows that the intensity of extreme precipitation is generally larger by 50% to 100% when the extreme precipitation is associated with LPS in central India.

The statistics of extremes can be also analyzed in terms of the duration of precipitation spells. A spell length refers to the amount of time for which precipitation on successive time instances exceeds a minimum specified value. Since IMD data is not available at sub-daily scale, 3-hourly TRMM precipitation data at $0.25^\circ \times 0.25^\circ$ resolution are used for analysis of precipitation spells. From the start date to the end date of a low pressure system, the locations which lie within 1000 km radii of the low pressure system track are considered and the time for which three-hourly precipitation is successively greater than 5 mm is calculated. The procedure is repeated for all LPS tracked during the study period (1998–2015), and the average spell length is calculated for each location (Fig. 13a). Maximum values of average precipitation spell length are found for locations along east and central Indian region. The values in the core monsoon region of central India are around 4.5–6 h, indicating that the extreme precipitation in these regions due to LPS are continuous in nature. The average amount of continuous rain occurring at a location which lies within 1000 km radii of LPS is shown in Fig. 13b. Large values can be seen in central India and the Gangetic plain. Our analysis of the duration of precipitation spell is limited by the coarser temporal resolution (3 h) of the TRMM precipitation data: the average spell lasts 3–6 h (Fig. 13), which is 1 to 2 TRMM timesteps. The use of hourly data would improve the accuracy of our spell length

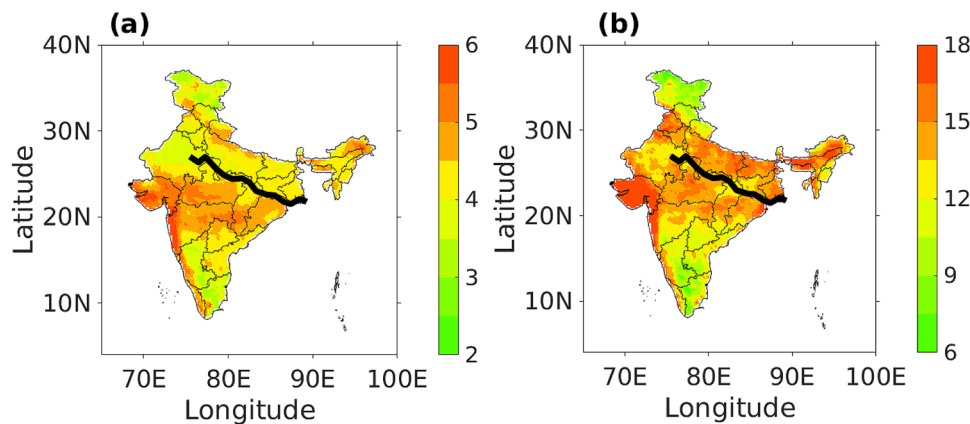


Fig. 13 Average precipitation spell length in hours **a** and average continuous precipitation in mm/3 h **b** for locations (within 1000 km radii of ATAGC based LPS tracks) by considering events observed during LPS days over the period 1998–2015 along with the median

LPS track (black solid line). TRMM 3B42V7 3-hourly precipitation data ($0.25^\circ \times 0.25^\circ$ resolution) are used for the analysis. A spell refers to the amount of time for which 3-hourly precipitation is greater than 5 mm

analysis. This is differed for future research using a higher temporal resolution dataset such as GPM-IMERG (Huffman et al. 2014).

Instead of the absolute thresholds used to define extreme precipitation events, some previous studies (e.g., Ajayamohan et al. 2010) have used percentile-based threshold to determine extreme precipitation events. When 98-percentile of daily precipitation is used as threshold for identifying extreme precipitation events, the total number of extreme events due to LPS (Fig. S17a) and the average number of extreme events per year due to LPS (Fig. S17a, b) are comparable to those determined by considering a fixed threshold (Fig. 10a, b) for grids in the study area. The spatial correlation between percentile-based extreme events and fixed threshold-based extreme events is 0.77 (Fig. 10a and Fig. S17a), indicating that the spatial patterns of number of extreme events determined by considering the two thresholds show some differences. However, the estimates of percentage of total extremes which are attributable to LPS (Fig. 10c and Fig. S17c) in analysis with both the thresholds have high (0.97) spatial correlation. Hence, it could be inferred that the results of our study are largely unaffected by the type of threshold used to estimate the extreme precipitation statistics.

5 Summary and conclusions

An algorithm (ATAGC) which uses geopotential criteria in addition to relative vorticity and winds for automated tracking of LPS has been developed. Its performance is analyzed by applying it on ERA-Interim reanalysis data and comparing the statistics of the obtained LPS tracks with those determined in previous studies.

In our analysis, around 14 systems per year are tracked with most of them originating in the northern BoB. These systems move north westwards with the median track covering the states of West Bengal, Odisha, Chhattisgarh, Jharkhand, Madhya Pradesh and Rajasthan (Fig. 2 and Fig. S11). Precipitation in these states crucially depends on the number and intensity of these LPS. The general location of genesis and tracks (in comparison with those available from previous studies) gives confidence in using our algorithm.

The correlation between the time series of annual frequency/number of systems (lows, depressions, deep depressions) identified using different LPS tracking algorithms is found to be low. This may be attributed to the subjectivity involved in identification and classification of the systems. Earlier studies (Sikka 2006; Ajayamohan et al. 2010) have shown a significant decline in the number of depressions and an increase in the number of lows. However, our analysis on ERA-Interim data using automated tracking algorithm (ATAGC) did not show any significant decline in the number

of depressions. This is in agreement with the findings of Cohen and Boos (2014).

A hundred percent coincidence probability is obtained between IMD and ATAGC based tracks of depressions over the period 1989–2003. Further, coincidence probability is greater than 50% between ATAGC and HB2015 based LPS tracks. Furthermore, spatial comparison of the ATAGC derived depression tracks with those found in IMD reports reveal that they are consistent with each other for the recent years (2010–2015).

Precipitation composites on LPS days and precipitation within 1000 km radii of the LPS tracks show large values over east and central India, which is in agreement with findings from earlier studies (Krishnamurthy and Ajayamohan 2010). Precipitation within 1000 km radii of ATAGC based LPS tracks is found to have large correlation (0.83) with that for HB2015 based LPS tracks. Similar results are obtained by analyzing precipitation composite. Overall, our analysis indicates that ATAGC algorithm can be used with confidence to arrive at reliable results.

Synoptic activity Index, which is a metric for LPS activity in terms of both number of systems and intensity, is found to be larger in northern BoB and in north-west direction over east and central India (core locations of LPS). However, trend in the annual value of this index is not statistically significant during 1979–2015.

Statistics of extreme precipitation events associated with LPS are also determined. Over the study period, we estimate that 27% area of the country experiences extreme precipitation associated with LPS, with about 12 extreme precipitation events per grid location per decade (on a $0.25^\circ \times 0.25^\circ$ grid). 15–25% of monsoon precipitation in east and central Indian region is in the form of extremes that are associated with LPS. At these locations, very heavy precipitation due to LPS has a return period less than 5 years. Further, the 99th percentile of extreme precipitation associated with LPS varies between 200 and 300 mm per day, while 95th percentile of extreme precipitation varies between 160 and 220 mm per day. The estimates are useful for assessing flood risk associated with LPS at various locations in central India for the monsoon season. The risk estimates are necessary for applications related to insurance assessment, and for general preparedness to mitigate adverse effects of LPS related extreme precipitation events.

The general characteristics of LPS have been captured by the ATAGC algorithm. But ATAGC as well as other algorithms show large differences in year-to-year variations in the frequency of LPS. However, the ability to identify all the major systems in recent years (2010–2015) is likely to make ATAGC more appealing for its use on GCM datasets for tracking LPS and analyzing changes in LPS characteristics in climate change scenarios. The proposed algorithm (ATAGC) could be readily used with outputs (vorticity,

geopotential, and temperature at 850 hPa) from climate models for determining future projections of LPS. However, an issue in such applications is that most of the CMIP5/6 GCMs don't provide future projections of vorticity. Nevertheless, climate model outputs on two variables (meridional and zonal wind components at 850 hPa) could be used to compute vorticity. Thus, the desired climate variables are readily available in most climate model outputs. Compared to ATAGC, the computational needs are less and scope for application to output from an ensemble of GCMs is more for algorithms which require only a few climate variables. For example, algorithm by Praveen et al. (2015) needs only one variable (sea level pressure).

The effect of orography cannot be neglected in analysis of extreme precipitation events related to LPS. Presence of mountain ranges outside the core LPS region (central and east India) should be also taken into account. By considering only the extreme events within 1000 km radii of LPS tracks (confined mainly to the central and northern parts of India), the statistics of extreme precipitation could not be assessed along Western Ghats (which lies outside the 1000 km radii) which receive large precipitation on LPS days. Incorporating such locations into the analysis is deferred for future research.

Acknowledgements The authors acknowledge all the organizations whose data were used in the present study, namely, European Center for Medium Range Forecasts, Tropical Rainfall Measuring Mission and India Meteorological Department. The first author acknowledges Ministry of Human Resource Development for fellowship provided through Prime Minister's Research Fellows Scheme. The second and third authors acknowledge the support from the Ministry of Earth Sciences through the Project MoES/PAMC/H&C/41/2013-PC-II.

Author contributions TMT, GB and SVV designed the study, TMT analyzed the data, and TMT, GB and SVV wrote the paper.

Funding Prime Minister's Research Fellows Scheme, Ministry of Human Resource Development, Government of India. Ministry of Earth Sciences, Project No. MoES/PAMC/H&C/41/2013-PC-II, Government of India.

Code availability Available through mailing to corresponding author.

Availability of data and material Available through mailing to corresponding author.

Compliance with ethical standards

Conflict of interest The authors declare no conflicts of interests or competing interests.

References

- Ajayamohan RS, Merryfield WJ, Kharin VV (2010) Increasing trend of synoptic activity and its relationship with extreme rain events over central India. *J Clim* 23(4):1004–1013. <https://doi.org/10.1175/2009JCLI2918.1>
- Blender R, Schubert M (2000) Cyclone tracking in different spatial and temporal resolutions. *Mon Weather Rev* 128(2):377–384
- Boos WR, Hurley J, Murthy V (2015) Adiabatic westward drift of Indian monsoon depressions. *Q J R Meteorol Soc* 141:1035–1048
- Chen TC, Yoon JH, Wang SY (2005) Westward propagation of the Indian monsoon depression. *Tellus A*. <https://doi.org/10.3402/tellusa.v57i5.14733>
- Cohen NY, Boos WR (2014) Has the number of Indian summer monsoon depressions decreased over the last 30 years? *Geophys Res Lett* 41(22):7846–7853. <https://doi.org/10.1002/2014GL061895>
- Dee DP, Uppala S, Simmons A, Berrisford P, Poli P, Kobayashi S et al (2011) The ERA-Interim reanalysis: configuration and performance of the data assimilation system. *Q J R Meteorol Soc* 137:553–597
- Dhar O, Nandargi S (1999) Role of low pressure areas in the absence of tropical disturbances during monsoon months in India. *Int J Climatol* 19(10):1153–1159. [https://doi.org/10.1002/\(SICI\)1097-0088\(199908\)19:10%3c1153::AID-JOC446%3e3.0.CO;2-C](https://doi.org/10.1002/(SICI)1097-0088(199908)19:10%3c1153::AID-JOC446%3e3.0.CO;2-C)
- Diaz M, Boos WR (2019) Barotropic growth of monsoon depressions. *Q J R Meteorol Soc* 145:824–844. <https://doi.org/10.1002/qj.3467>
- Gadgil S (2003) The Indian monsoon and its variability. *Ann Rev Earth Planet Sci* 31(1):429–467
- Goswami BN (1987) A mechanism for the west-north-west movement of monsoon depressions. *Nature* 326(6111):376–378. <https://doi.org/10.1038/326376a0>
- Goswami BN, Ajayamohan RS, Xavier PK, Sengupta D (2003) Clustering of synoptic activity by Indian summer monsoon intra-seasonal oscillations. *Geophys Res Lett* 30:1431. <https://doi.org/10.1029/2002GL016734>
- Goswami BN, Venugopal V, Sengupta D, Madhusoodanan MS, Xavier PK (2006) Increasing trend of extreme rain events over India in a warming environment. *Science* 314(5804):1442–1445. <https://doi.org/10.1126/science.1132027>
- Hersbach H, Dee D (2016) ERA5 reanalysis is in production, ECMWF Newsletter 147, ECMWF, Reading, UK
- Hersbach H, Bell W, Berrisford P, Hor'anyi AJ, M-S, Nicolas J, et al (2019) Global reanalysis: goodbye ERA-Interim, hello ERA5. 17–24.
- Hodges KI (1994) A general method for tracking analysis and its application to meteorological data. *Mon Weather Rev* 122(11):2573–2586. [https://doi.org/10.1175/1520-0493\(1994\)122%3c2573:AGMFTA%3e2.0.CO;2](https://doi.org/10.1175/1520-0493(1994)122%3c2573:AGMFTA%3e2.0.CO;2)
- Huffman G, Bolvin D, Braithwaite D, Hsu K, Joyce R, Xie P (2014) Integrated Multi-satellite Retrievals for GPM (IMERG), version 4.4. NASA's Precipitation Processing Center, accessed 31 March, 2015, <ftp://arthurhou.dds.eosdis.nasa.gov/gpmdata/>.
- Hunt KMR, Fletcher JK (2019) The relationship between Indian monsoon rainfall and low-pressure systems. *Clim Dyn* 53(3):1859–1871. <https://doi.org/10.1007/s00382-019-04744-x>
- Hunt KMR, Parker DJ (2016) The movement of Indian monsoon depressions by interaction with image vortices near the Himalayan wall. *Q J R Meteorol Soc* 142:2224–2229
- Hunt KMR, Turner AG (2017) The effect of horizontal resolution on Indian monsoon depressions in the Met Office NWP model. *Q J R Meteorol Soc* 143:1456–1771
- Hunt KMR, Turner AG, Inness PM, Parker DE, Levine RC (2016) On the structure and dynamics of Indian monsoon depressions. *Mon Weather Rev* 144(9):3391–3416. <https://doi.org/10.1175/MWR-D-15-0138.1>
- Hurley JV, Boos WR (2015) A global climatology of monsoon low-pressure systems. *Q J R Meteorol Soc* 141(689):1049–1064. <https://doi.org/10.1002/qj.2447>

- IITM M ESSO (2015) A research report on the 2015 southwest monsoon. ISSN 0252–1075, ESSO/IITM/SERP/SR/02(2015)/185:23–33
- IMD (2003) Cyclone manual.
- IMD (2011) Monsoon 2010. IMD Met Monograph. Synoptic Meteorology No: 10/2011:21–47
- IMD (2012) Monsoon 2011. IMD Met Monograph. Synoptic Meteorology No: 01/2012:17–30
- IMD (2013) Monsoon 2012. IMD Met Monograph. Synoptic Meteorology No: 13/2013:15–46
- IMD (2014) Monsoon 2013. IMD Met Monograph. ESSO Document No:ESSO/IMD/Synoptic Met./01(2014)/15:10–13
- IMD (2015) Monsoon 2014. IMD Met Monograph. ESSO Document No:ESSO/IMD/Synoptic Met./01(2015)/17:08–13
- Karmakar N, Chakraborty A, Nanjundiah RS (2017) Increased sporadic extremes decrease the intraseasonal variability in the Indian summer monsoon rainfall. *Sci Rep* 7:7824. <https://doi.org/10.1038/s41598-017-07529-6>
- Keshavamurty RN, Satyan V, Goswami BN (1978) Indian summer monsoon cyclogenesis and its variability. *Nature* 274(5671):576–578. <https://doi.org/10.1038/274576a0>
- Krishnamurti TN, Kanamitsu M, Godbole R, Chang CB, Carr F, Chow JH (1975) Study of a monsoon depression (i). *J Meteorol Soc Japan Ser II* 53(4):227–240. https://doi.org/10.2151/jmsj1965.53.4_227
- Krishnamurthy V, Ajayamohan RS (2010) Composite structure of monsoon low pressure systems and its relation to Indian rainfall. *J Clim* 23(16):4285–4305. <https://doi.org/10.1175/2010JCLI2953.1>
- Krishnamurthy CK, Lall U, Kwon H (2009) Changing frequency and intensity of rainfall extremes over India from 1951 to 2003. *J Clim* 22:4737–4746. <https://doi.org/10.1175/2009JCLI2896.1>
- Krishnan R, Ayantika DC, Kumar V, Pokhrel S (2011) The long-lived monsoon depressions of 2006 and their linkage with the Indian Ocean Dipole. *Int J Climatol* 31:1334–1352. <https://doi.org/10.1002/joc.2156>
- Mandke SK, Bhide UV (2003) A study of decreasing storm frequency over Bay of Bengal. *J Ind Geophys Uni* 7:53–58
- Meera M, Suhas E, Sandeep S (2019) Downstream and in situ: two perspectives on the initiation of monsoon low-pressure systems over the Bay of Bengal. *Geophys Res Lett* 46:12303–12310. <https://doi.org/10.1029/2019GL084555>
- Mooley DA, Shukla J (1987) Characteristics of the westward-moving summer monsoon low pressure systems over the Indian region and their relationship with the monsoon rainfall. College Park, University of Maryland, Department of Meteorology, Center for Ocean–Land–Atmosphere Interactions, 47
- Nigam S, Baxter S (2015) General circulation of the atmosphere. In: Gerald RN, John P, Fuqing Z (eds) Encyclopedia of atmospheric sciences (Second Edition, 9–109) Academic Press. <https://doi.org/10.1016/B978-0-12-382225-3.00400-X>.
- Patwardhan SK, Bhalme HN (2001) A study of cyclonic disturbances over India and the adjacent ocean. *Int J Climatol* 2:527–534. <https://doi.org/10.1002/joc.615>
- Praveen V, Sandeep S, Ajayamohan RS (2015) On the relationship between mean monsoon precipitation and low-pressure systems in climate model simulations. *J Clim* 28(13):5305–5324. <https://doi.org/10.1175/JCLI-D-14-00415>
- Prajeesh AG, Ashok K, Rao DVB (2013) Falling monsoon depression frequency: a gray-Sikka conditions perspective. *Sci Rep*. <https://doi.org/10.1038/srep02989>
- Prakash S, Sathiyamoorthy V, Mahesh C, Gairola RM (2014) An evaluation of high-resolution multisatellite rainfall products over the Indian monsoon region. *Int J Rem Sens* 35(9):3018–3035. <https://doi.org/10.1080/01431161.2014.894661>
- Rastogi D, Ashfaq M, Leung LR, Ghosh S, Saha A, Hodges K, Evans K (2018) Characteristics of Bay of Bengal monsoon depressions in the 21st century. *Geophys Res Lett* 45(13):6637–6645. <https://doi.org/10.1029/2018GL078756>
- Rajeevan M, Bhate J, Kale JD, LaL B (2006) High resolution daily gridded rainfall for the Indian region: analysis of break and active rain spells. *Curr Sci* 91:296–306
- Rajeevan M, Bhate J, Jaswal AK (2008) Analysis of variability and trends of extreme rainfall events over India using 104 years of gridded daily rainfall data. *Geophys Res Lett*. <https://doi.org/10.1029/2008GL035143>
- Saha KR, Mooley DA, Saha S (1979) The Indian monsoon and its economic impact. *GeoJournal* 3(2):171–178. <https://doi.org/10.1007/BF00257706>
- Samet H (1981) Connected component labeling using quadtrees. *J ACM* 28(3):487–501. <https://doi.org/10.1145/322261.322267>
- Sandeep S, Ajayamohan RS, Boos WR, Sabin TP, Praveen V (2018) Decline and poleward shift in Indian summer monsoon synoptic activity in a warming climate. *Proc Natl Acad Sci* 115(11):2681–2686. <https://doi.org/10.1073/pnas.1709031115>
- Sikka DR (1977) Some aspects of the life history, structure and movement of monsoon depressions. *Pure Appl Geophys* 115(5):1501–1529. <https://doi.org/10.1007/BF00874421>
- Sikka DR (1980) Some aspects of the large-scale fluctuations of summer monsoon rainfall over India in relation to fluctuations in the planetary and regional scale circulation parameters. *Proc Indian Acad Sci* 89(2):179–195. <https://doi.org/10.1007/BF02913749>
- Sikka DR (2006) A study on the monsoon low pressure systems over the Indian region and their relationship with drought and excess monsoon seasonal rainfall. Center for Ocean–Land–Atmosphere Studies, Tech Rep 217:61
- Sørland SL, Sorteberg A (2016) Low-pressure systems and extreme precipitation in central India: sensitivity to temperature changes. *Clim Dyn* 47(1):465–480. <https://doi.org/10.1007/s00382-015-2850-4>
- Vishnu S, Boos WR, Ullrich PA, O’Brien TA (2020) Assessing historical variability of South Asian monsoon lows and depressions with an optimized tracking algorithm. *J Geophys Res: Atmos* 125:e2020JD032977. <https://doi.org/10.1029/2020JD032977>
- Webster P (1987) The elementary monsoon. *Monsoons* eds. Wiley, New Jersey

Publisher's Note Springer Nature remains neutral with regard to jurisdictional claims in published maps and institutional affiliations.